

Simulation of Heat Effected Zone in Welding Process and Characterization of Arc, MIG and TIG Welding Methods

A. Akshay Kumar¹, D.V.Pareshwar², Sainath Kasuba³

¹Student, Dept. of Mechanical Engineering, Sreyas Institute of Engineering & Technology, Hyderabad, India

²Asst. Prof., Dept. of Mechanical Engineering, Sreyas Institute of Engineering & Technology, Hyderabad, India

³Assoc. Prof., Dept. of Mechanical Engg., Sreyas Institute of Engineering & Technology, Hyderabad, India

Abstract—The application of the ferrous alloys plays the key role in the manufacturing industry. The process of joining techniques and their effect on the metallurgical properties of the metal greatly effects the strength of the joint and the life of the product. In the current project the three different types of welding techniques i.e. Tungsten Inert gas, Metal Inert gas and Arc welding are performed on AISI 1024 .The effect of these three types of techniques on the series of steel alloys is tested by destructive techniques. The microstructure, hardness and tensile strength at the joints, HEZ and base plate are evaluated.

Index Terms—AISI 4130, AISI 4140, AISI 4330, TIG, MIG, ARC, Heat Effected Zone

I. INTRODUCTION

The heat supplied by a welding arc produces complex thermal cycle in the weldment and leads to creation of transient thermal stresses, and finally results in the creation of residual stresses in the weldment. The extent of this heating, in turn, affects the degree and nature of residual stresses in the newly joined assembly. The temperature history of the welded components also has a significant influence on the residual stresses. The control of these temperature fields and cooling rates is essential to ensure low residual stresses. The measurement of surface temperatures during fission welding is difficult, fairly complex and requires specialized equipment.

Therefore, recourse is to use quantitative calculations to gain insight into the phenomenon of heat transfer during fusion welding. Theoretical analysis of the weld thermal cycle usually requires number of simplifying assumptions regarding the material properties of the melt and the high temperature properties of the base metal. Arc efficiency is also an important parameter to measure the efficiency of heat transfer during arc welding processes. For all these reasons analysis of distribution of heat and transient temperature cycle in fusion welds is needed. In the weld pool, heat is transported by means of conduction and convection. Convective heat flow in welding cannot be accurately solved analytically because of its complexity; as a result the heat flow calculations made so far are limited to simplified heat conduction calculations.

Important aspects to note are as follows: (a) The temperature starts at the ambient temperature of the environment prior to the arrival of a moving heat source (b) the temperature rises very rapidly once the heat source acts on the point (c) the temperature reaches a maximum or "peak" determined by the balance between the energy being inputted and all losses (d) the temperature remains at that maximum only as long as the source remains on that spot (which, for a moving source, is only an instant) (e) the temperature cools back to the ambient level at a rate dependent on the thermal mass and thermal-physical properties of the material and any imposed cooling.

II. LITERATURE SURVEY

A. Experimental Evaluation of Mechanical Properties

In the present analysis AISI 1024 5 mm thickness plates were used for the analysis and the schematic model of weld preparation is given below.

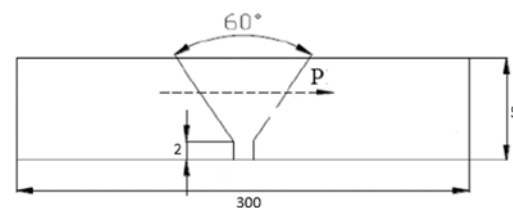


Fig. 1. Welding sample preparation

B. Specimen Preparation

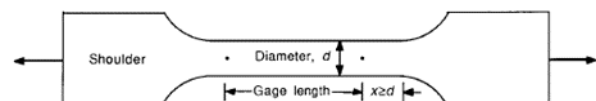


Fig. 2. Tensile test specimen as per ASME SEC-IX: 2017

The test specimens of 5mm thickness were welded using Electric ARC, TIG and MIG with a single V groove as shown in the above figure. The filler material have melting point less than that of the parent metal and are more elastic than the parent metal therefore they prevent cracking in TIG welding with . The

metals are welded with the filler metal used is ER70S for TIG welding, ER70S-3 electrode for MIG welding, E6010 electrode for ARC welding.

1) Microstructure

The Microstructure of the base plate, weld bead are examined for the evaluation of the other properties. The etchant is used as NITAL 2% (HNO₃ diluted with alcohol).

C. Mechanical Property Evaluation

1) Tensile test

All the tensile properties for base plate were evaluated as per the standard IS 1608:2005 and for the all the weld specimens the test standards are carried as per the ASME standard ASME SEC-IX: 2017. The tensile test specimen configuration is shown in Fig. 2 .The specimens were carefully machined using a wire cut electrical discharge machine. The test was carried out using a FIE 40 UTN-40 universal testing machine. The properties like ultimate tensile strength, percentage of elongation, proof stress and load were determined by using load displacement data obtained during the test.

2) Microstructure

In order to identify the variation of properties in base metal, weld regions on specimens, microstructure analysis was carried out as per the ASTM standard E 407. For the welded specimen the microstructure analysis were carried out at the fracture zone.

3) Hardness

The standard Vickers hardness test was conducted on both weld regions as well as parent metal according to the standard specified by IS 1501:2002.This test was carried out using diamond indenter and load applied is equal to 10 kgs.

III. RESULTS AND DISCUSSIONS

A. Tensile Test Results

The tensile strength was evaluated for all the weld specimens. The Table-1, clearly shows that the base material is having significantly high ultimate tensile strength as compared to that of weld bead specimens. This value is 168% high as compared to arc weld specimen nearly 18% higher than GTAW specimen and nearly 82.3% higher than GTAW specimen.

B. Test Specimen for Tensile Test



Fig. 3. Specimen of (a) Base plate (b) Arc Welding (c) TIG welding (d) MIG Welding

C. Tensile Test Graph of Base Metal

In the Fig. 4, the displacement i.e. strain on the specimen is increased linearly with the load until 95 kN and then it attained yield point and got fractured at 89.1 kN.

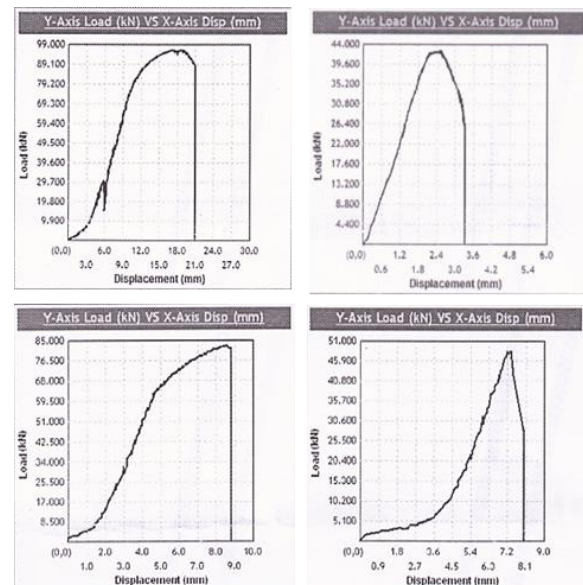


Fig. 4. Tensile test graph of base metal, ARC, TIG & MIG welded sample

D. Tensile Test Graph of TIG Welded Sample

Initially the specimen undergone strain linearly and the sample go fractured at 85 kN without any plasticity.

E. Tensile Test Graph of MIG Welded Sample

Initially the specimen undergone strain linearly and the sample go fractured at 47 kN approximately without any plasticity.

TABLE I
 TENSILE TEST RESULTS OF ALL THE THREE TYPES OF WELDING SPECIMENS

Specimen	Ultimate load	Ultimate tensile strength	Elongation %	Yield load	Yield stress	Original gauge length	Final gauge length
	KN	N/mm ²					
Base Material	96	906.088	16.98	85.82	809.981	58.17	68.05
Arc weld specimen	41.2	337.125	-	-	-	-	-
GTAW specimen	82.56	765.721	6.12	63.8	591.727	59	62.61
MIG Specimen	48.48	496.82	4.82	45.47	468.744	56	58.7

F. Microstructure

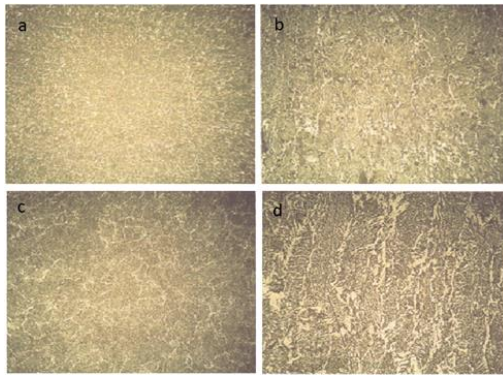


Fig. 5. Microstructure images of various joint zones (a) Base metal (b) Arc Welding (c) TIG welding (d) MIG Welding

The microstructure consists of two eutectoid ferrite in the matrix of ferrite. The matrix contains fine grains of ferrite.

The weld bead of arc welded specimen weld zone consists of columnar grains with grain boundary as ferrite and windmanstatten ferrite in the matrix of pearlite.

The microstructure of TIG welded specimen consists of fine grains of grain boundary ferrite with some windmanstatten ferrite and polygon ferrite in the matrix of ferrite

Microstructure of MIG weld zone consists of coarse columnar grains with grain boundary ferrite and windmanstatten ferrite in the matrix of pearlite.

G. Hardness Test

Vickers hardness values are evaluated for all the three specimens (base metal, GTAW weld bead, FSW weld bead).The result shows that GTAW weld bead hardness is marginally higher as compared to that of base metal and FSW weld bead. The hardness values are presented in the Table.

H. Study of Heat effected Zone by thermal Analysis

The present research work concentrates on the how the heat transfer is taking place when an arc welding torch is being moved on the weld area of the plates. For the current analysis two plates of dimensions 200*150*5 mm AISI 1020 plates are taken and simulated for the thermal distribution.

I. Material Properties

For the convenience of the simulation half symmetry model is considered for the analysis. Standard weld bead geometry and gap between the two weld plates is maintained as per the ASME welding standards.

TABLE II
MATERIAL PROPERTIES

Property	Value
Density	8000 g/cc
Young's modulus	190 GPa
Poisson's ratio	0.29
Tensile strength	320 Mpa
Thermal conductivity	46 W/m-k

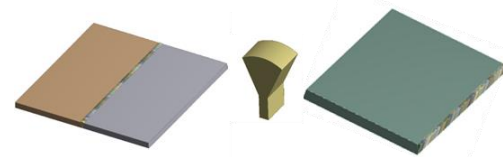


Fig. 6. Complete geometry of weld specimen, Weld bead geometry & Symmetry model

J. Meshing

The model has been meshed with the required element size and the mesh method.



Fig. 7. Mesh model

Boundary Conditions:

The boundary conditions are calculated for the present model using some set of relations.

Boundary conditions needed:

- Heat source calculation.
- Convection parameters.

Heat source calculations:

$$\text{Heat input} = \frac{V \times I}{T}$$

Where,

$$V - \text{Voltage} = 21V$$

$$I - \text{Amperes} = 165A.$$

$$\text{Heat input} = \frac{V \times I}{T} = \frac{165 \times 21}{0.38 \times \frac{1}{60}} = 0.54 \text{ kJ/mm}$$

$$\text{Arc travel time} = 0.38 \text{ m/min}$$

$$= \frac{380}{60}$$

$$= 6.3 \text{ mm/sec}$$

$$\text{Wattage} = \text{Heat input} * T \text{ mm/sec}$$

$$= 0.54 * 6.3$$

$$= 3.402 \text{ kJ/sec}$$

TABLE III
ARC WELDING PARAMETERS

CTWD: 1/2" (13mm)															
Plate Thickness(mm)	0.6		0.9		1.5		2		3		4		5		6
Electrode Dia (mm)	0.6	0.8	0.8	0.9	0.8	0.9	0.8	0.9	0.8	0.9	0.8	0.9	1.1	1.1	1.1
WFS - (M/min)	2.5	1.9	3.2	2.5	4.4	3.8	5.7	4.4	7	5.7	7.6	6.4	3.2	3.8	5
Amps (approximate)	35	35	55	80	80	120	100	130	115	160	130	175	145	165	200
Travel Speed (M/min)	0.25	0.25	0.35	0.33	0.33	0.5	0.45	0.45	0.5	0.5	0.43	0.5	0.45	0.3=	0.33
Voltage	17	17	18	18	19	19	20	20	21	21	22	22	18-20	19-21	20-22

= 3.402 kW

$$Gr = \frac{g \cdot L^3 \cdot \beta \cdot (T_p - T_a)}{\eta^2}$$

$$\beta = \frac{1}{T_a}, 1/K$$

= 3402 W

Internal generation per unit volume = $\frac{\text{Wattage}}{\text{Volume of weld bead}}$

$$= \frac{3402}{17.668}$$

$$= 192.5 \text{ W/mm}^3$$

Transient Time Step:

The complete weld run is divided into 50 domains throughout the weld run with a domain size of 3mm.

The analysis is carried out for every 0.5sec and heat input is given as per the time step.

Time travel = 0.38 m/min = 6.3 mm/sec

Total time for welding 150mm is 23.08sec and it is rounded to

$$Pr = \frac{\mu \cdot Cp}{k}$$

25 sec

For each bead the heat is made to generate for 0.5sec and rest the heat is allowed to conduct to the plate.

Convection:

For convection we use the convection heat transfer coefficient h_c , W/(m² K). A different approach is to define h through the Nusselt number Nu , which is the ratio between the convective and the conductive heat transfer:

$$Nu = \frac{\text{Convective heat transfer}}{\text{Conductive heat transfer}} = (h_c \cdot L) / k$$

Where:

- Nu = Nusselt number
- h_c = convective heat transfer coefficient
- k = thermal conductivity, W/mK
- L = characteristic length, m

The convection heat transfer coefficient is then defined as following:

The Nusselt number depends on the geometrical shape of the heat

$$h_c = \frac{Nu \cdot k}{L}$$

sink and on the air flow. For natural convection on flat isothermal plate the formula of Na is given in Table-4

TABLE IV
 NUSSELT NUMBER FORMULA

	Vertical fins		Horizontal fins
Laminar flow	$Nu = 0.59 \cdot Ra^{0.25}$	Upward laminar flow	$Nu = 0.54 \cdot Ra^{0.25}$
Turbulent flow	$Nu = 0.14 \cdot Ra^{0.33}$	Downward laminar flow	$Nu = 0.27 \cdot Ra^{0.25}$
		Turbulent flow	$Nu = 0.14 \cdot Ra^{0.33}$

Where:

$$Ra = Gr \cdot Pr$$

is the Rayleigh number defined in terms of Prandtl number (Pr) and Grashof number (Gr). If $Ra < 106$ the heat flow is laminar, while if $Ra > 106$ the flow is turbulent.

The Grashof number, Gr is defined as following:

Where:

- g = acceleration of gravity = 9.81, m/s²

- L = 0.130, longer side of the fin, m
 - β = air thermal expansion coefficient. For gases, is the reciprocal of the temperature in Kelvin:

$\beta = 0.033$

- $T_p = 75^\circ\text{C}$, Plate temperature, $^\circ\text{C}$.

- $T_a = 30^\circ\text{C}$, Air temperature, $^\circ\text{C}$

- η = air kinematic viscosity, $1.6 \cdot 10^{-5}$ at 30°C .

$$Gr = \frac{9.81 \cdot 0.130 \cdot 0.130 \cdot 0.130 \cdot 0.033 \cdot (75 - 30)}{1.6 \cdot 10^{-5}^2}$$

$$Gr = 7.2 \cdot 10^7$$

For plate temperature, T_p , set a expected value. Finally, the Prandtl number, Pr is defined as:

Where:

- μ = air dynamic viscosity, is $1.86 \cdot 10^{-5}$ at 30°C .

- c_p = air specific heat = 1005 J/(Kg \cdot K) for dry air

- k = air thermal conductivity = 0.026 W/(m \cdot K) at 30°C

$$Pr = \frac{1.86 \cdot 10^{-5} \cdot 1005}{0.026}$$

$$Pr = 0.7189$$

Convective heat transfer coefficient:

$$h_c = \frac{57.59 \cdot 0.026}{0.130}$$

$h_c = 11.874$ (For vertical walls)

$h_c = 10.864$ (For horizontal walls)

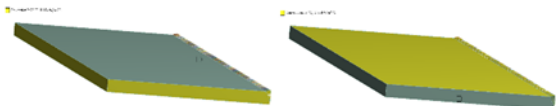


Fig. 8. Convection for vertical walls and horizontal walls

K. Simulation Results

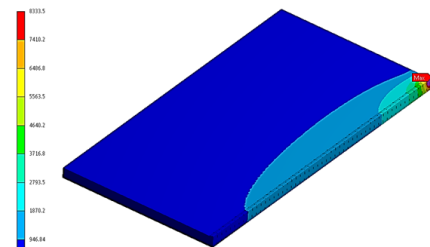


Fig. 9. Temperature contour of the welding simulation at the end of simulation

L. Graph

The below graph depicts the temperature distribution with respect to the time, the temperature of 11000°C is achieved for the fraction of time at 25 sec, whereas a maximum temperature of 8000°C is observed at every weldment of the specimen between 3 to 24 seconds.

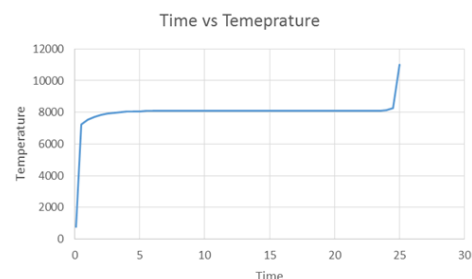


Fig. 10. Time vs. Temperature

IV. CONCLUSION

In the present analysis the primary investigation is done to determine the thermal distribution due to the heat source on the material and it is simulated by using the Ansys thermal package. The heat source energy is calculated using the correlations of the input voltage, current and weld transverse speed. The maximum temperature attained is in the order of 8333°C and minimum temperature is 946.84°C.

In the present analysis, the material grade AISI 1024 is joined by using three different welding techniques namely ARC Electrode welding, Tungsten Inert Gas welding (TIG) and Metal Inert Gas welding (MIG). The mechanical properties are evaluated using destructive techniques to compare the weld bead strength among the techniques mentioned above. The samples are prepared as per the standards and the microstructure, hardness, tensile properties are compared.

The ultimate tensile strength of base plate i.e. 906MPa is comparatively higher than other specimens, from the weld specimens the TIG specimen have higher tensile strength i.e. 765.721 MPa compared to MIG specimen i.e. 496.820 MPa and Arc weld specimen has lowest strength i.e. 337.120 MPa, this may be due to the post weld heat treatment. The Arc weld specimen failed immediately without any change in the gauge length as a result of heat treatment.

The hardness of TIG weld specimen i.e. 268.67 HV is comparatively higher than other samples due to the fine grains of ferrite in the matrix of pearlite and MIG weld specimen has the lowest value of 195 HV due to the coarser grains.

The microstructure of the both base metal and the TIG weld specimen has finer grains of pearlite in the matrix of ferrite. Other two specimens microstructure differs with the columnar coarse grains with ferrite boundary in the matrix of pearlite.

REFERENCES

- [1] P. S. Myers, O. A. Uyehara, and G. L. Borman, "Fundamentals of Heat Flow in Welding," Welding Research Council Bulletin No. 123, July 1967.
- [2] R. F. Jones, Jr., H. Armen, and J. T. Fong, Eds., Numerical Modeling of Manufacturing Processes, ASME Publication PVP-PB-025, November 1977.
- [3] N. S. Boulton and H. E. Lance Martin, "Residual Stresses in Arc Welded Plates," Proc. Inst. Mech. Engrs., Vol. 133, 1936, pp. 295-339.
- [4] D. Rosenthal and R. Schnerber, "Thermal Study of Arc welding," - Welding Journal, Research Supplement, Vol. 17, No. 4, April 1938.
- [5] L. Tall, "Residual Stresses in Welded Plates - A Theoretical Study," Welding Journal, Research Supplement, Vol. 43, No. 1, January 1964, pp. 10s-23s.
- [6] H. D. Hibbitt and P. V. Marcal, "A Numerical Thermo-Mechanical Model for the Welding and Subsequent Loading of a Fabricated Structure," Computers and Structures, Vol. 3, No. 5, September 1973, pp. 1145-1174.
- [7] S. S. Glickstein, "Arc Modeling for Welding Analysis," WAPD-TM-1382, Bettis Atomic Power Laboratory, April 1978.
- [8] E. Friedman, "On the Calculation of Temperatures Due to Arc Welding," in Computer Simulation for Materials Applications, R. J. Arsenault, J. R. Beeler, Jr., and J. A. Simmons, Eds., Nuclear Metallurgy, Vol. 20, Part 2, April 1976, pp. 1160-1170.
- [9] D. Rosenthal, "The Theory of Moving Sources of Heat and Its Application to Metal Treatments," -Trans. ASME, Vol. 68, 1946, pp. 849-866.
- [10] R. J. Grosh, E. A. Trabant, and G. A. Hawkins, "Temperature Distribution in Solids of Variable Thermal Properties Heated by Moving Heat Sources," Q. Appl. Math., Vol. 13, No. 2, 1955, pp. 161-167.
- [11] T. Naka and K. Masubuchi, "Temperature Distribution of Welded Plates," J. Japan Welding Soc., Vol. 16, Nos. 7 and 12, 1947, pp. 281-290, 374-378.
- [12] E. Friedman, "Thermo-mechanical Analysis of the Welding Process Using the Finite Element Method," Trans. ASME, J. Pressure Vessel Techn., Vol. 97, Series J, No. 3, August 1975, pp. 206-213.
- [13] E. L. Wilson and R. E. Nickell, "Application of the Finite Element Method to Heat Conduction Analysis," Nuclear Engr. and Design, Vol. 4, 1966, pp. 276-286.
- [14] E. Friedman, "An Iterative Procedure for Including Phase Change in Transient Heat Conduction Programs and Its Incorporation Into the Finite Element Method," Proc. 17th National Heat Transfer Conf., AIChE, August 1977, pp. 182-187.
- [15] C. Zienkiewicz, The Finite Element Method in Engineering Science, McGraw-Hill, London, 1971.
- [16] S. S. Glickstein and w.' Yeniscavich, "A Review of Minor Element Effects on the Welding Arc and Weld Penetration," Welding Research Council Bulletin No. 226, May 1977.
- [17] S. S. Glickstein and E. Friedman, "Temperature and Distortion Transients in Gas Tungsten-Arc Weldments," WAPD-TM-1428, Bettis Atomic Power Laboratory, October 1979.
- [18] E. Friedman, "Numerical Simulation of the Gas Tungsten-Arc Welding Process," in Numerical Modeling of Manufacturing Processes, ASME Publication PVP-PB-025, November 1977, pp. 35-47
- [19] T. Muraki, J. J. Bryan, and K. Masubuchi, "Analysis of Thermal Stresses and Metal Movement During Welding," Trans. ASME, J. Engr. Materials and Techn Vol. 97, Series H, No. 1, January 1975, pp. 81-91.
- [20] E. Friedman and S. S. Sattinger, "Temperatures and Distortions Induced by Omega Seal Closure Welding," ASME Paper No. 70WA/PVP~O, December 1976.
- [21] W.F. Hosford, Overview of Tensile Testing, Tensile Testing, P. Han, Ed., ASM International, 1992, p 1-24
- [22] P.M. Mumford, Test Methodology and Data Analysis, Tensile Testing, P. Han, Ed., ASM International, 1992, p 49-60
- [23] Iterative calculation of the heat transfer coefficient, D.Roncati Progettazione Ottica Roncati, via Panfilio, 17 - 44121 Ferrara.